Molecular Therapy
Nucleic Acids
Original Article

DNA aptamers that modulate biological activity of model neurons

Jenelle Rolli,[1,8] Keenan Pearson,[1,8] Brandon Wilbanks,[1,2] Sybil C.L. Hrstka,[7] Andrew P. Minotti,[3,4,5] Lorenz Studer,[3,4,5] Arthur E. Warrington,[6] Nathan P. Staff,[7] and L. James Maher III[1]

[1]Department of Biochemistry and Molecular Biology, Mayo Clinic College of Medicine and Science, Rochester, MN 55905, USA; [2]Biochemistry and Molecular Biology Track, Mayo Clinic Graduate School of Biomedical Sciences, Rochester, MN 55905, USA; [3]The Center for Stem Cell Biology, Sloan-Kettering Institute for Cancer Research, New York, NY 10065, USA; [4]Developmental Biology Program, Sloan-Kettering Institute for Cancer Research, New York, NY 10065, USA; [5]Weill Graduate School of Medical Sciences of Cornell University, New York, NY 10065, USA; [6]Department of Neurologic Surgery, Mayo Clinic, Rochester, MN 55905, USA; [7]Department of Neurology, Mayo Clinic, Rochester, MN 55905, USA

There is an urgent need for agents that promote health and regeneration of cells and tissues, specifically to treat diseases of the aging nervous system. Age-associated nervous system degeneration and various diseases are driven by many different biochemical stresses, often making it difficult to target any one disease cause. Our laboratory has previously identified DNA aptamers with apparent regenerative properties in murine models of multiple sclerosis by selecting aptamers that bind oligodendrocyte membrane preparations. Here, we selected from vast libraries of molecules ($\sim 10^{14}$ unique DNAs) those with the ability to bind cultured human SH-SY5Y neuroblastoma cells as a neuronal model, followed by screening for aptamers capable of eliciting biological responses, with validation of binding in differentiated SH-SY5Y, human induced pluripotent stem cell (iPSC)-derived sensory neurons, and human embryonic stem cell (hESC)-derived cortical neurons. This demonstrates a proof-of-concept workflow to identify biologically active aptamers by cycles of cell selection.

INTRODUCTION

The etiologies of neurodegenerative diseases vary widely even within a single disease category, and many of these diseases share genetic links and patterns of molecular pathogenesis. This variability in etiology raises the possibility of generic disease treatment by stimulating cell health, resilience, and regeneration, ideally countering neurodegeneration stemming from a wide range of causes. Approaches that seek to promote cell regeneration have been undertaken utilizing stem cells, antibodies, and nucleic acid aptamers. There are several stem cell-based therapies currently undergoing clinical trials (NCT03280056, NCT03268603, NCT03482050). These therapies have the goal of neuroprotection through paracrine effects rather than the replacement of lost neurons. One approach relies on autologous mesenchymal stem cells (MSCs) for their ability to secrete neurotrophic factors and modulate the immune system.[1–3] Various strategies are being implemented to increase neurotrophic factor secretion by such MSCs, including conditioned media and gene editing to drive overexpression.[4,5] Another approach uses neuroglial lineage precursors.[6,7] However, the allogeneic nature of this formulation requires concomitant immunosuppression.

Certain natural human immunoglobulin (Ig)M antibodies have been identified for their ability to bind neurons and elicit regenerative responses.[8–17] A recombinant form of one such human IgM, rHIgM22, was shown to promote central nervous system (CNS) remyelination in models of multiple sclerosis (MS),[9–11,14,17,18] a disease in which the myelin sheath coating neuronal axons is damaged. Based on the results reported for rHIgM22, our laboratory developed DNA aptamers LJM-3064 and LJM-5708 by cycles of selection for binding to rodent CNS myelin suspensions.[18] We then studied their pharmacodynamics and delivery to the CNS of mice after intraperitoneal (i.p.) injection of these DNA aptamers.[19] When biotinylated and multimerized around a streptavidin core, formulations of these aptamers showed features reminiscent of rHIgM22, promoting myelin regeneration and functional improvement in a Theiler's murine encephalomyelitis virus (TMEV) mouse model of progressive MS.[10,18–21] An independent study showed efficacy of a different formulation of this DNA aptamer in an experimental autoimmune encephalomyelitis (EAE) mouse model of MS.[22] This work demonstrates the potential for selection of biologically active DNA aptamers by affinity selection against disease-relevant targets.

Another neuron-binding human antibody reported to elicit regenerative responses is rHIgM12. This molecule has been shown to increase neuron attachment in culture and promote neurite outgrowth.[12,16] rHIgM12 was further evaluated for *in vivo* efficacy in two SOD1 mouse models of amyotrophic lateral sclerosis (ALS).[15] A single dose of rHIgM12 was reported to increase survival, reduce symptom progression, reduce myelin whorls (indicative of degenerating axons),

Received 7 April 2024; accepted 12 November 2024;
https://doi.org/10.1016/j.omtn.2024.102392.

[8]These authors contributed equally

Correspondence: L. James Maher, Department of Biochemistry and Molecular Biology, Mayo Clinic College of Medicine and Science, 200 First St SW, Rochester, MN 55905, USA.
E-mail: maher@mayo.edu

and increase the number of spinal cord anterior horn cells (indicating a reduction in motor neuron degeneration) in mice.[15] Such results might translate into increased human ALS patient survival.

As demonstrated by antibody screens, large libraries of affinity molecules may be needed to identify a small number that can elicit desired biological responses. We demonstrate here a workflow that can eventually be applied to any cultured cell model. This proof-of-concept study initially exploits SH-SY5Y neuroblastoma cells as an example because of their relevance to unmet needs in neurological diseases and oncology.[23–25] We then extend the work to mature human brain neurons. Based on cell culture assays of growth, morphology, elicited transcriptional responses, and protein induction, we describe several DNA aptamers that modulate biological activity in these neuron models.

RESULTS

Aptamer selection

We set out to determine if DNA aptamers can be identified with the ability to elicit potentially useful biological responses in neurons. Our strategy was to identify cell-binding DNA aptamers by *in vitro* selection, characterize and quantitate binding specificity, and then screen for biological activity. To do this, cultured adherent SH-SY5Y cells were first used as a convenient neuron model for positive selection and non-neuronal cells as negative-selection targets to identify SH-SY5Y-specific DNA aptamers using the three similar approaches described in materials and methods (Figure 1A). The progress of each selection was monitored by subjecting recovered aptamer libraries to qPCR.[26] In general, library recovery increased across selection rounds (Figure S1). The original naive library (denoted selection round 0) and libraries from various selection rounds were subjected to next-generation sequencing. Top sequences were identified based on their enrichment over rounds of selection, indicated by their abundance (Figures 1B–1D). The proportion of non-unique sequences increased over the course of each selection (Figure S2).

We chose 41 unrelated sequences from the top candidates identified in each of the three similar selections (Figure 1) using AptaSUITE.[27] These candidates were synthesized individually with 3′-biotin tags and screened for the ability to specifically bind model neurons (Figure 2; Table S1). We also chose negative-control sequences 6699 and 6953 that were present in the original naive selection libraries but not in any of the rounds of selection (Table S1). The predicted secondary structures of all candidates were generated using Mfold and the predicted free energies of the negative-control oligonucleotides were within the range of those for the candidate aptamers (Table S2).[28,29]

Aptamer binding

We assessed the binding of all candidate aptamer sequences and controls to SH-SY5Y cells by image analysis. SH-SY5Y cells were seeded and grown overnight to the same density as in the selection (Figure 2 inset). Aptamer staining was performed and quantified as described in materials and methods. Three previously described DNA aptamers were included along with the candidate aptamers and controls described above. First, we included a previously published aptamer from our laboratory, 3064, which had been selected against rodent CNS myelin suspension.[18] Another aptamer, yly12, was reportedly selected against neurites isolated from differentiated SH-SY5Y cells but also bound undifferentiated SH-SY5Y cells. This aptamer reportedly binds L1CAM.[30] The third aptamer, Apt3, was reported to bind to poly-sialic acid and was of interest because neuroregenerative antibody rHIgM12 reportedly binds to poly-sialic acid-modified NCAM.[13,31] All candidates were synthesized with 3′ terminal biotin tags allowing detection of cell-specific binding by fluorescently labeled streptavidin following incubation on cultured cells, washing to remove unbound molecules, and formaldehyde fixation. Twenty-four candidate aptamers, including all those previously published, exhibited statistically significant staining of SH-SY5Y cells compared to both negative-control oligonucleotides (Figures 2 and S3). Eighteen of the 21 candidate aptamers exhibiting statistically significant staining of SH-SY5Y cells compared to both negative controls and showed no statistically significant staining of the respective negative-selection cell line when compared to a negative-control oligonucleotide (Figure S4). We found that pre-conjugation of biotinylated aptamers with fluorescent streptavidin resulted in optimal staining, so we optimized the ratio of aptamer to streptavidin to minimize free aptamer and maximize higher-order multimers (Figure S5). The staining of several aptamers was confirmed by high-resolution confocal microscopy using the optimized pre-conjugation method (Figure S6).

We sought to optimize certain aptamers by truncation to reduce their size, aiming to minimize production costs and facilitate future development efforts. We used Mfold to predict the secondary structures of 10 aptamers.[28] Truncations were then designed to remove apparently unstructured terminal regions. In most cases, the truncated aptamers performed equally relative to full-length molecules, except for 7088, 7085, and 7086, where the truncated versions significantly diminished staining compared with their full-length counterparts (Figure 3).

We next tested whether the aptamers selected against undifferentiated SH-SY5Y cells would also bind to their differentiated counterparts. We consider differentiated SH-SY5Y cells to represent a more mature neuron model. A standard protocol for the differentiation of SH-SY5Y cells was used and aptamer binding was assessed at the end of the 11-day induction.[32] Differentiated SH-SY5Y cells exhibited an obvious increase in the number and length of neurite-like processes potentially establishing contacts between cells (Figures S7 and S9 inset). β3-Tubulin, GAP43, and Tau staining was performed and quantified showing a statistically significant increase in β3-tubulin and Tau, supporting the successful differentiation of the SH-SY5Y cells (Figure S8). Seventeen of the aptamers that bound undifferentiated cells also exhibited statistically significant staining of differentiated SH-SY5Y cells compared to both negative-control oligonucleotides (Figures S9 and S10). The staining of several aptamers was confirmed by high-resolution confocal microscopy using the optimized pre-conjugation method (Figure S11).

We tested the ability of several of the top aptamers to bind more mature neuronal cultures by using induced sensory neurons (iSNs)

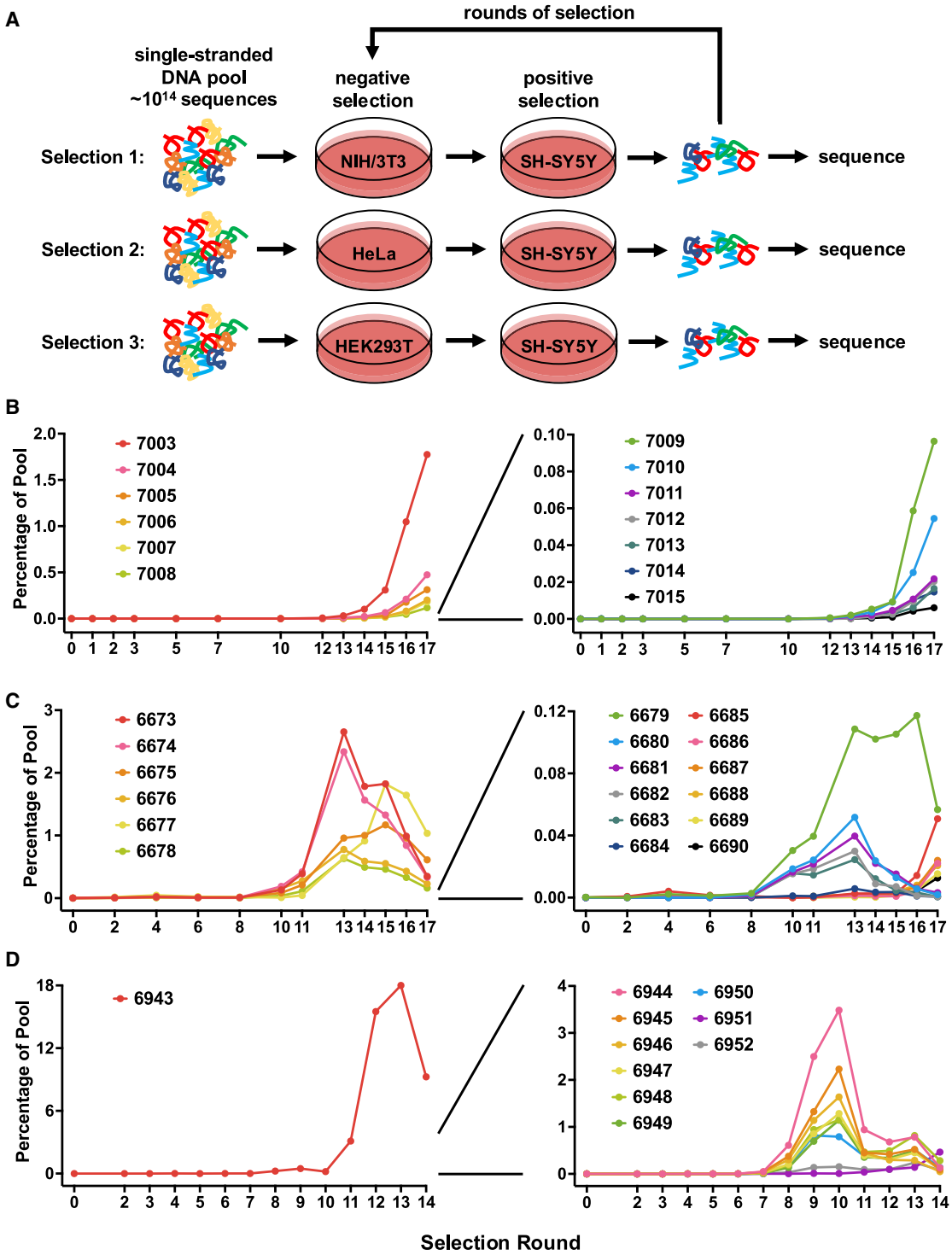

Figure 1. Selection of DNA aptamers that bind SH-SY5Y cells

(A) Schematic of selection procedure showing negative-selection cell lines used for selections 1, 2, and 3. (B–D) Prevalence of the indicated candidate from deep-sequencing data is shown across rounds of selections 1–3, respectively. Panels on right expand the y axis for clarity.

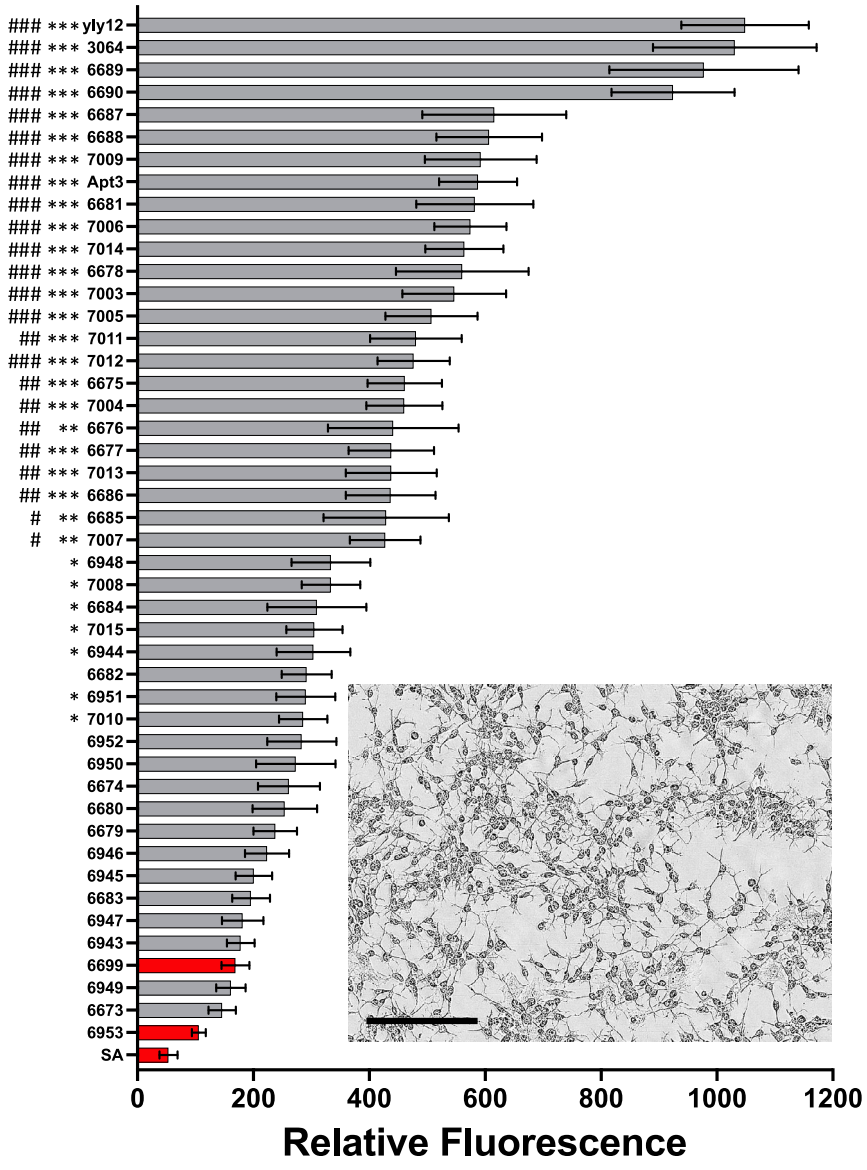

Figure 2. Screening candidate aptamers by assessing binding to SH-SY5Y cells

Phase-contrast image to show cell morphology of proliferating SH-SY5Y cells at 20× magnification; scale bar, 200 μm (inset). Binding quantification for candidates (7003–7015, 6673–6690, and 6943–6952), other published aptamers (3064, yly12, and Apt3), and negative controls (6699, 6953, and streptavidin only [SA]; bars shown in red). Quantification of staining was calculated as NIR signal intensity per image field normalized to confluence (as described in section materials and methods). Statistical significance is shown for comparison with 6699 (#$p < 0.05$, ##$p < 0.01$, ###$p < 0.001$) and 6953 (*$p < 0.05$, **$p < 0.01$, ***$p < 0.001$) by one-way ANOVA. Data are represented as mean ± SEM for multiple image fields (n = 34–78). Image analysis was performed with IncuCyte SX5.

derived from human induced pluripotent stem cells (iPSCs). Two published aptamers (yly12 and 3064) along with three of the candidate aptamers from the SH-SY5Y selections (6681, 6689, and 6690) showed specific staining of iSNs when compared with a negative-control oligonucleotide (Figure S12). Quantification of this staining is made difficult by the morphological complexity of these neuronal cultures, so representative confocal images are shown without statistical comparison.

Biological assays

After identifying aptamers that bound to target cells, we performed a colony-formation assay with the SH-SY5Y neuroblastoma cells to observe any long-term effects of aptamer treatment on cell growth. In this assay, we interpret colony formation as a primary readout of biological activity, including positive or negative growth effects or inducing differentiation. We hypothesize that aptamers that inhibit colony formation may do so by toxic or differentiation effects; however, colony-formation counts do not differentiate such responses. The focus of this assay was to narrow our list of candidates with potential biological activity. We observed after 14 days of treatment with 200 nM aptamer that seven candidates altered with statistical significance the ability of SH-SY5Y cells to form colonies. Two candidates increased colony formation and five decreased colony formation relative to a negative control (Figures 4A and S13). Because pre-conjugation of biotinylated aptamers with streptavidin had appeared to improve staining results, we tested whether multimerizing biotinylated aptamers with streptavidin would modify the biological response in the colony-formation assay. The biological effect of yly12, the aptamer that most effectively inhibited colony formation, was abrogated by multimerization with streptavidin (Figure S14). We next sought to optimize the concentration of aptamer for maximum effect on colony formation. A dose-response study showed a minor growth-inhibitory effect due to the negative control observed at 500 nM, but not at 350 nM (Figure S15). We therefore used 350 nM aptamer for further testing. To check whether this activity was specific to SH-SY5Y cells, we performed the colony-formation assay with two of the negative-selection cell lines. Only 7083 showed any activity, a statistically significant *inhibition* of HeLa cell colony formation, opposite to its activity on SH-SY5Y cells (Figure S16). NIH/3T3 cells did not form colonies and could not be tested in this assay.

The colony-formation assay measured response to aptamer treatment on sparsely plated model cells over a time frame of 14 days. We tested

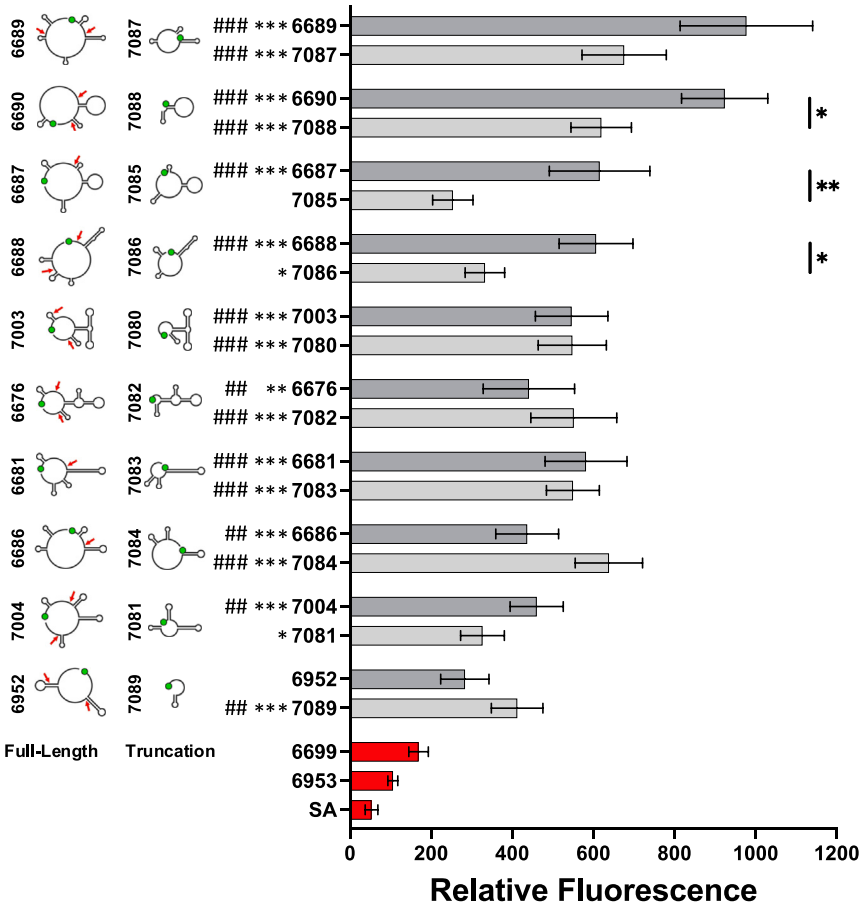

Figure 3. Screening truncated aptamers by assessing binding to SH-SY5Y cells

Schematic representations of predicted secondary structures for full-length aptamers and truncations determined using Mfold. Green circle indicates the 5′ terminus. Red arrows indicate truncation positions within full-length sequences. Binding quantification of full-length aptamers are shown in the top of each bar grouping (dark gray), and quantification of truncations are shown in the bottom of each bar grouping (light gray). Statistical significance is shown for comparison with 6699 (#$p < 0.05$, ##$p < 0.01$, ###$p < 0.001$) and 6953 (*$p < 0.05$, **$p < 0.01$, ***$p < 0.001$) by one-way ANOVA. Data are represented as mean ± SEM for multiple image fields. Data for full-length aptamers and negative controls are the same as shown in Figure 2.

aptamer effects on more densely plated cells over a shorter period (5 days) to prevent the culture reaching maximum confluence. Cell confluence was measured after 5 days of treatment, and while the general trend was the same as seen in the colony-formation assay, only 7083 showed a statistically significant increase in confluence compared to a negative-control oligonucleotide (Figure 4B). The observed reduction in growth over a shorter treatment window reflects the time required to induce differentiation, typically requiring weeks rather than days.[33–35] Since adherent SH-SY5Y cells in culture have short neurite-like processes, we quantified the effect of aptamer candidates on fold change in process length per cell cluster count and process branches per cell cluster count. Aptamer 7089 showed a statistically significant increase in both morphological measurements when compared to negative-control 6699. This is remarkable given the typical timeline of neural differentiation in cell culture (Figures 4C and 4D). Phase-contrast images and corresponding process and cluster masks are shown in Figure 4E.

The biological activity findings prompted follow-up with an RNA-sequencing (RNA-seq) study to determine gene expression changes in undifferentiated SH-SY5Y cells after 5 days of treatment with a subset of aptamers. All seven candidate aptamers that affected colony formation induced statistically significant changes in gene expression when compared with the negative-control oligonucleotide. Aptamer 7004 showed the most pronounced response (Figures 5A and S17). Gene Ontology (GO) analysis of up- and downregulated genes in 7004-treated cells revealed many GO terms related to neuronal function (Figures 5B and 5C). It is notable that many GO terms associated with metabolism and growth were significant when analyzing both the downregulated and upregulated genes from 7004-treated samples (Figures S18 and S19). Gene set enrichment analysis (GSEA) revealed two hallmarks from the 7004-treated sample data: oxidative phosphorylation and DNA repair (Figures 5D and S20). Several GO terms also appear to be associated with oxidative phosphorylation when the genes upregulated by 7004 treatment were analyzed (Figure 5E), while no GO terms were associated with DNA repair. Differential expression of neuronal genes resulted in significant GO pathways, including synapse structure, axonogenesis, neurogenesis, and oxidative phosphorylation. Such changes have previously been associated with neuron differentiation.[34] Notably, these differentiation-related changes were observed just 5 days after aptamer treatment, while negative-control oligonucleotide treatment induced no such response. While the other six aptamers showed statistically significant changes in gene expression levels, GO analysis and GSEA did not reveal any significant terms (Figure S17). These other aptamers might be activating signaling networks that are not detected by gene expression alone at this particular treatment concentration and time point. These results constitute the first evidence that a rapid biological response is elicited in a neuron model by sequence-specific aptamer interactions.

We next examined whether 7004 could induce any biological effect on cortical neurons derived from human embryonic stem cells (hESCs). High-content imaging analysis showed 7004 bound to cortical neurons with higher affinity than 6699, the negative-control oligonucleotide, at all aptamer concentrations tested (Figure S21). We then

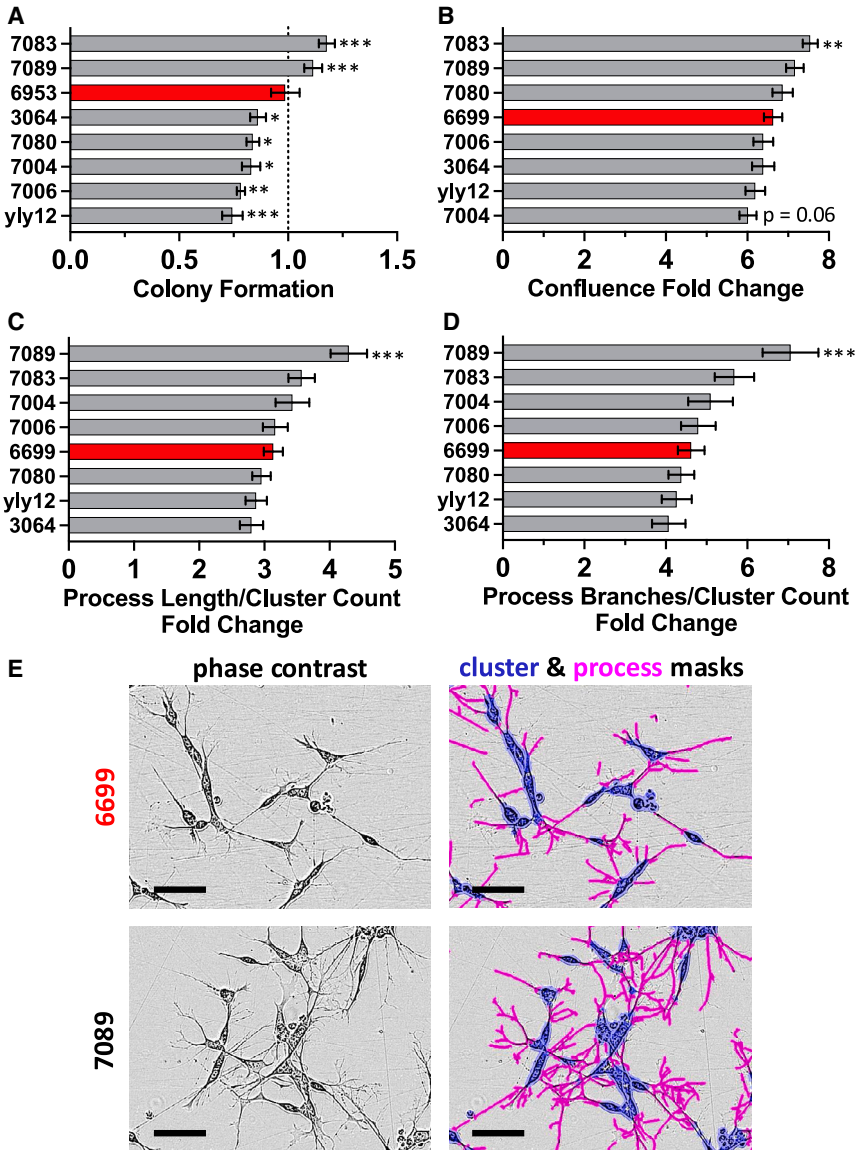

Figure 4. Aptamer treatment effects in cell culture

(A) Daily treatment with 200 nM aptamers (gray) identifies those that promote or inhibit SH-SY5Y colony formation when compared to identical treatment with negative-control oligonucleotides (red). Colony formation is compared to treatment with control oligonucleotides. Statistical significance is shown for comparison with 6953 (*p < 0.05, **p < 0.01, ***p < 0.001) by one-way ANOVA. Data are represented as mean ± SEM for biological replicates (n = 4). (B–D) Daily treatment with 350 nM aptamers (gray) identifies aptamers that promote increased confluence (B), neurite length per cluster count (C), and neurite branches per cluster count (D) when compared to identical treatment with a negative-control oligonucleotide (red). Statistical significance is shown for comparison with 6699 (*p < 0.05, **p < 0.01, ***p < 0.001) by one-way ANOVA. Data are represented as mean ± SEM for biological replicates (n = 46–48). (E) Example regions of images quantified for (C) and (D). The cluster mask is shown in blue, and the process mask is shown in pink. Scale bars, 100 μm.

tested whether 7004 influenced induction of FOS, an immediate-early gene upregulated in response to various stimuli in the nervous system.[36] Indeed, we found that neurons treated with 7004, but not negative-control 6699, exhibited a dose-dependent increase in nuclear FOS signal intensity, indicating a stimulatory effect on the cortical neurons (Figure 6). We also investigated whether this result was due to an innate immune response by quantifying the translocation of nuclear factor κB (NF-κB) from the cytoplasm to the nucleus. This result shows no indication of NF-κB activation, suggesting a sequence-specific stimulatory effect of 7004 treatment on cortical neurons that is not due to an innate immune response (Figure S22).

DISCUSSION

This work describes a workflow for the selection and characterization of DNA aptamers with the potential to elicit biological responses in model neurons. We performed three different selections with varying conditions (e.g., temperature, competitor, negative-selection cell line). We varied the temperature to either encourage cell surface receptor binding (4°C) or physiological interactions (37°C). While the degree of surface binding is not determined in this work, all binding assays were performed at 37°C and aptamers selected at 4°C bound to a similar extant to those selected at 37°C. We varied the non-specific competitor and again there was not a large difference between those aptamers selected with sheared salmon DNA present or yeast tRNA present. We used three different negative-selection cell lines to steer aptamer selections away from common surface molecules shared by target and non-target cells. While comparison is complicated by the other varied selection conditions, the only selection that selected lead aptamers completely specific for target cells was selection 3 using HeLa cells (Figure S4). Although it is not feasible to test every combination of conditions with an identical library in replicates, we chose to vary the conditions to produce a diverse collection of aptamers to begin screening for biological activity. Aptamers that elicited biological responses were either full length or truncations found from across all three selections.

This process led to the collection of 41 DNA aptamers displaying varying degrees of affinity for growing and differentiated SH-SY5Y cells. Of this collection, almost 20% (7 out of 41) were found to induce changes in SH-SY5Y cell colony formation and gene expression detectable by RNA-seq. While we have used a series of low-throughput biological assays in our workflow, we envision possible improvements. For

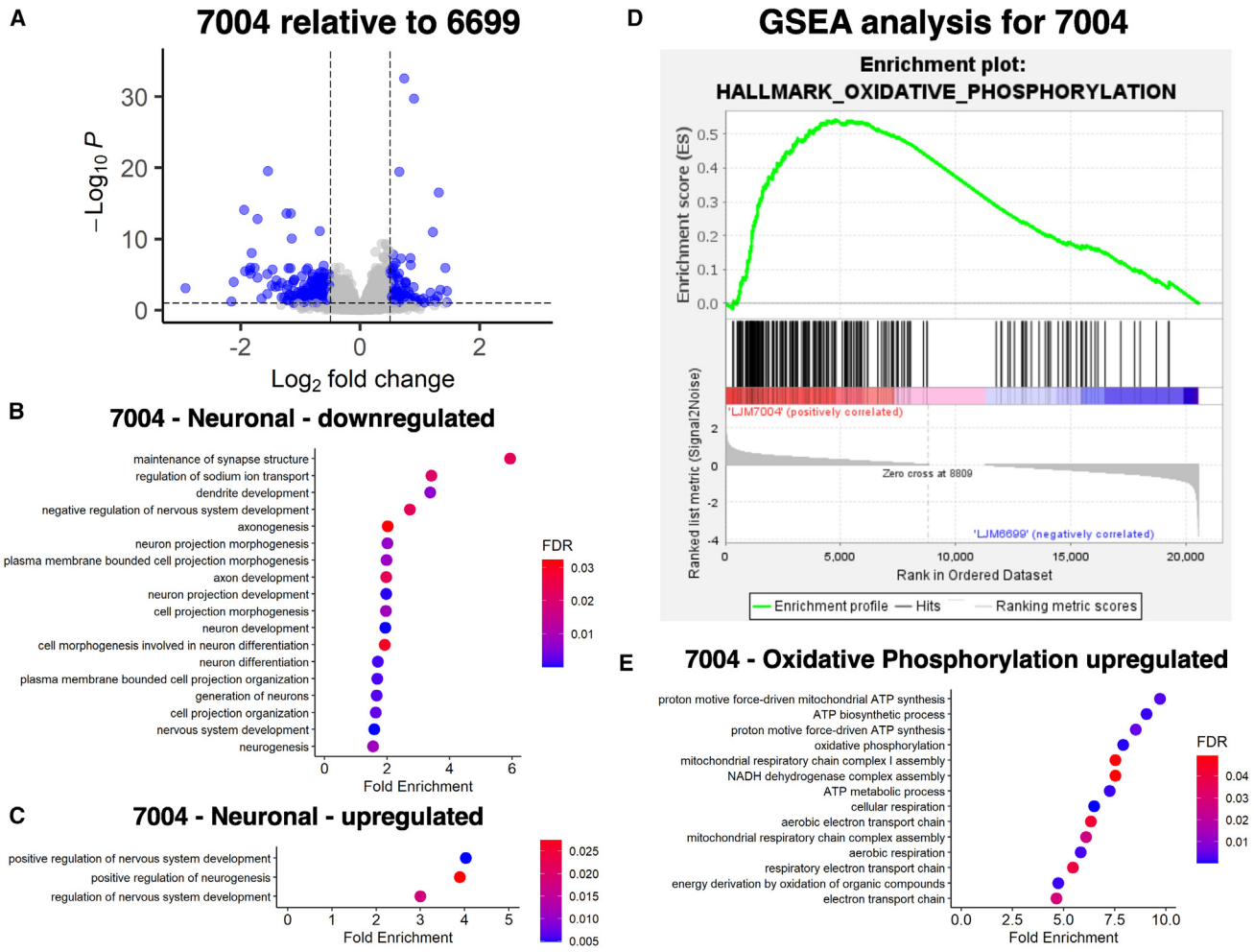

Figure 5. Gene expression changes after SH-SY5Y treatment with 7004

(A) RNA-seq analysis of total RNA collected from cultures treated with aptamer (7004) or control oligonucleotide (6699). Log_2 fold change was calculated as a ratio of 7004:6699. (B and C) Neuronal Gene Ontology (GO) terms resulting from analysis of downregulated (B) and upregulated (C) genes after treatment with 7004. (D) Gene set enrichment analysis (GSEA) revealed enrichment in oxidative phosphorylation for 7004. (E) GO terms associated with oxidative phosphorylation were upregulated after treatment with 7004.

example, a high-throughput workflow could be applied to a large number of selected aptamers identified by deep sequencing without any need for cell affinity confirmation or characterization. In the future, it would be appropriate to expand this concept to explore libraries of selected DNA aptamers for biological activity in approaches similar to those taken with small molecules.[34] Further, a high-throughput biological activity assay would also allow for varying levels of streptavidin multimerization to more easily be tested.

We note that, in the present work, we successfully leveraged cell replication rates and colony formation by proliferating model neurons as a powerful aspect of our screen for biological activity. This strategy is obviously limited to proliferating cells prior to differentiation. However, measuring DNA aptamer effects on colony formation by undifferentiated SH-SY5Y neuroblastoma cells provides a powerful, inexpensive, and sensitive screening step in our proposed workflow to identify bioactive DNA aptamers that influence the biology of mature neurons. Although CNS neurons are post-mitotic, many of the signaling pathways relevant to aptamer effects on cell division rate of neuron-like precursors remain relevant in post-mitotic neurons. Aptamers that inhibit colony formation could be toxic or could have this effect by promoting differentiation. This can be discerned in subsequent more sophisticated and expensive screening assays, as we have shown. Furthermore, discovering influences of DNA aptamers on growth of non-differentiated neuron model cells is highly relevant to strategies involving iPSC-derived neurons where modification of differentiation pathways remains an unmet research and therapy need.

Our results indicate that 7004 triggers biological activity that is in some ways reflective of neuron differentiation. Some responses to

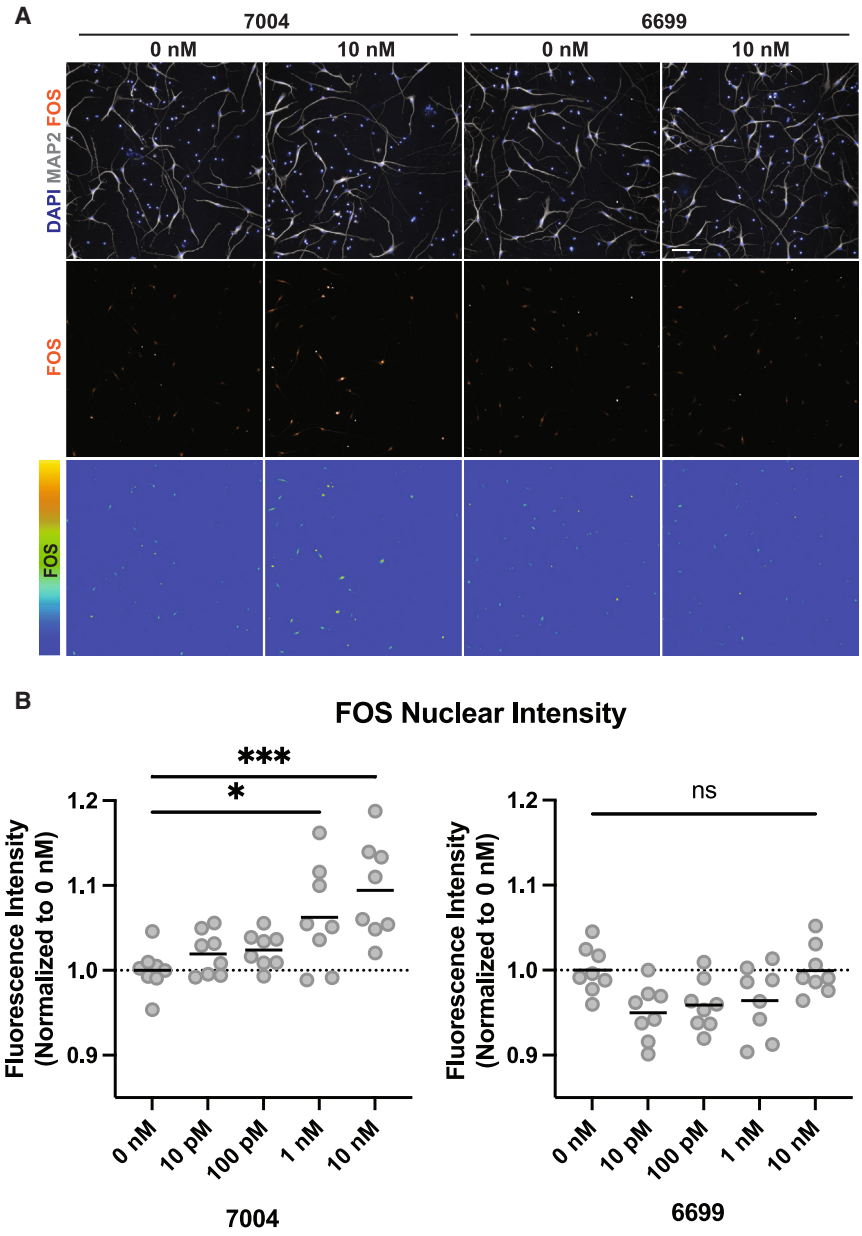

Figure 6. Induction of nuclear FOS after hESC-derived cortical neuron treatment with 7004

(A) Representative images of immunofluorescent staining of hESC-derived cortical neurons treated with aptamer 7004 and negative-control oligonucleotide 6699 at 20× magnification. Scale bar, 100 μm (inset). Markers include DAPI, microtubule-associated protein-2 (MAP2), and FOS. (B) Quantification of FOS nuclear signal intensity (n = 8 wells) is displayed relative to the mean intensity of the untreated control. Mean values are represented by a black line. Two-tailed student's t test; asterisks indicate statistical significance (*$p < 0.05$, ***$p < 0.001$).

7004 treatment are consistent with maturation of neuronal processes, most strongly supported by a shift toward oxidative phosphorylation. 7004 is therefore a candidate for further study as a neuroregenerative therapeutic agent potentially capable of promoting differentiation of iPSCs into mature neuronal cells.

Treatment of neurodegenerative diseases may require lifelong therapy, and applications such as supporting nerve grafts after surgery also require extended periods of time. A hydrogel delivery system has been shown to provide a sustained release of aptamer.[37] This hydrogel system suggests a slow-release approach to deliver aptamers to neural targets over weeks to months required for regeneration of injured nerves.

SH-SY5Y cells are often used as model neurons, and therefore this collection of aptamers may find other useful applications in neuroscience. While these cells represent perhaps an unusual neuron model, their facile culture has allowed for them to be studied for decades as useful surrogates. Here, their properties facilitated straightforward selections to be performed before screening candidate aptamers on cultures with more relevant neuron-like phenotypes.[38] SH-SY5Y cells are also a useful model of neuroblastoma tumors, so this same collection of aptamers may possibly be useful leads for anti-proliferative therapeutics or cell-targeted drug delivery agents against neuroblastoma.

This work demonstrates a plausible workflow for future DNA aptamer selections against living cells or tissues to identify candidates that can then be screened for desired biological activity. As mentioned in the introduction, screens of natural human antibodies have been performed with this same approach in mind. However, since they must first be screened for affinity, the number of candidates for a biological activity screen can be severally limited. The selection of DNA aptamers finds candidates with affinity for the cells of interest and can produce a large library of affinity molecules to screen for biological activity. Additionally, we demonstrate an example biological activity workflow, but any desirable biological activity assay can be inserted for the application of interest. We envision possible future studies in which aptamers are selected against various mature neurons to identify neuroregenerative oligonucleotides. iPSC-derived neuron models can be generated from patient-derived cells to identify aptamers that act specifically on diseased target cells. Further, aptamers capable of promoting specific differentiation outcomes might be identified by performing selections against naive iPSCs.

MATERIALS AND METHODS

Cell culture

SH-SY5Y cells were cultured in DMEM:F12 medium (Gibco, 11330057) with 10% fetal bovine serum (FBS) (R&D Systems, S11550H) and 1% penicillin-streptomycin (Gibco, 15140122). HeLa and HEK293T cells were cultured in DMEM (Gibco, 11965118) with 10% FBS (R&D Systems, S11550H) and 1% penicillin-streptomycin (Gibco, 15140122). These cells were maintained at 20% oxygen and 5% CO_2.

Buffers

Wash buffer is DPBS (Gibco, 14190-144) containing 5 mM $MgCl_2$ and 4.5 g/L glucose. Binding buffer contains 5 mM $MgCl_2$, 4.5 g/L glucose, 100 μg/mL tRNA, and 100 μg/mL BSA. 2× PK buffer contains 100 mM Tris-HCl (pH 7.5), 200 mM NaCl, 2 mM EDTA, and 1% SDS. 0.5× TBE buffer contains 45 mM Tris-borate, pH 8.0, and 1 mM EDTA.

Oligonucleotides

DNA library, primers, and aptamers were purchased from Integrated DNA Technologies (Coralville, IA) with standard desalting. All sequences and abbreviations are provided in Table S1.

DNA aptamer selections

Three different selections (S1–S3) were performed. The protocol described below notes variations between selection conditions.

SH-SY5Y cells were cultured to ∼80% confluency on untreated 10-cm tissue culture dishes (Falcon, 353003) (S1, 4 million plated 24 h prior for first round and 2.25 million for subsequent rounds; S2 and S3, 2.5 million plated 48 h in advance with a medium exchange at 24 h). Negative-selection cells were cultured to ∼80% confluency as above (S1, no negative selection for rounds 1–2 and then plated 1 million NIH/3T3 cells 24 h prior for subsequent rounds; S2, no negative selection for rounds 1–2 and then plated 250,000 HeLa cells 48 h prior for subsequent rounds; S3, 1.5 million HEK293T cells for the first round and 750,000 cells for subsequent rounds plated 48 h in advance). 80-nucleotide (nt) naive DNA libraries (40 central random nt flanked by blocks of 20 defined nt for PCR priming) were purchased from Integrated DNA Technologies (Coralville, IA) with standard desalting. For round 1, 1 nmol (∼6×10^{14} molecules) random DNA library (S1 and S2, library 6014; S3, library 6857) was prepared in 2 mL of wash buffer, heated at 90°C for 5 min, and snap cooled on ice. Nonspecific competitors were then added (S1, fragmented salmon sperm DNA [100 μg/mL] and BSA [1 μg/mL]; S2 and S3, tRNA [100 μg/mL] and BSA [100 μg/mL]). Subsequent rounds employed DNA library recovered and purified from large-scale (2 mL) PCR amplification (S1, 200 pmol for rounds 2–11 and 100 pmol for rounds 12–17; S2 and S3, 100 pmol). Medium was aspirated from negative-selection cells (when applicable) and the dish was rinsed once with DPBS. The library solution was added to the negative-selection cells and incubated (S1, 4°C for 30 min in rounds 3–4 and for 60 min in rounds 5–17; S2, 37°C for 30 min in rounds 3–17; S3, 37°C for 30 min). Medium was aspirated from SH-SY5Y cells and the dish was rinsed once with DPBS. When indicated, library solution was transferred from the negative-selection cells to the SH-SY5Y cells and incubated (S1, 4°C for 60 min; S2, 37°C for 30 min; S3, 37°C for 30 min). For S1, SH-SY5Y cells were scraped into binding buffer, collected by centrifugation, and washed three times by centrifugation (500 × *g* for 5 min). For S2 and S3, SH-SY5Y cells were washed on the dish three times with wash buffer, scraped into wash buffer, and collected by centrifugation (500 × *g* for 5 min). The supernatant was removed, and the cell pellet was resuspended in 500 μL of wash buffer. Cells were lysed by heating at 95°C for 10 min. For S1 and S2, debris was removed by centrifugation at 13,100 × *g* for 5 min, and the supernatant containing the recovered library was moved to a fresh tube. For S3, the lysate was extracted with an equal volume of phenol:chloroform:iso-amyl alcohol (25:24:1) (VWR, 97064-692), and the upper aqueous phase was then precipitated from ethanol.

For the first selection round, the cell pellet was lysed in water rather than wash buffer and the extract from the entire cell pellet was used as the template for 1 mL of PCR with the following reagent volumes: 500 μL round 1 lysate, 100 μL of 10× PCR buffer, 80 μL of 2.5 mM deoxyribonucleotide triphosphates (dNTPs), 100 μL of 1 mg/mL BSA, 80 μL of 50 mM $MgCl_2$, 50 μL of forward primer (S1 and S2, 5304; S3, 6638) (10 μM stock), 50 μL of reverse primer (S1 and S2, 6015; S3, 6858) (10 μM stock), 20 μL of water, 20 μL of Taq (Invitrogen, 10342178). The mixture was split into 100-μL aliquots and subjected to thermal cycling (S1 and S2, 95°C for 60 s, 8 × [95°C, 30s; 70°C, 90s]; S3, 94°C for 60 s, 8 × [94°C, 30 s; 52°C, 35 s; 72°C, 30 s]).

The lysate (or the PCR product from the first round) was used directly as a template for analytical PCR to determine the optimum number of cycles to be used in a large-scale PCR. The following reagent volumes were used: 200 μL of template, 200 μL of 10× PCR buffer, 160 μL of 2.5 mM dNTPs, 200 μL of 1 mg/mL BSA, 160 μL of 50 mM $MgCl_2$, 200 μL of forward primer (S1 and S2, 5304; S3, 6638) (5 μM stock), 200 μL of reverse primer (S1 and S2, 6015; S3, 6858) (5 μM stock), 652 μL of water, and 28 μL of Taq. The mixture was split into 100-μL aliquots and subjected to thermal cycling following the protocol described above with the optimum number of cycles as determined with analytical PCR followed by sample electrophoresis.

Following amplification, aliquots were recombined. 3 M NaOAc was added and mixed (0.1 volumes). Nucleic acids were precipitated by the addition of 2.5 volumes of ethanol, mixing, incubation on dry ice for 15 min, and centrifugation at 17,000 × *g* for 15 min. The pellet was washed with 70% ethanol followed by centrifugation at 17,000 × *g* for 5 min. The pellet was air dried, resuspended in 40 μL of water, combined with 160 μL of deionized formamide, heated at 90°C for 5 min, loaded onto a 10% denaturing polyacrylamide gel (7.5 M urea, 19:1 acrylamide:bisacrylamide), and subjected to electrophoresis for 2.5 h at 600 V (26.25 V/cm).

Bands were visualized with a handheld UV lamp. The higher-mobility DNA band containing the fluorescent single-stranded library was excised using a clean razor blade. This material was cleaved into small

cubes and eluted overnight at 37°C in 500 μL of 2× PK buffer on an end-over-end rotator. The supernatant was extracted against an equal volume of phenol:chloroform:iso-amyl alcohol (25:24:1) (VWR, 97064-692). The upper aqueous phase was then precipitated from ethanol as described above. The pellet was resuspended in 100 μL of water. The concentration of the library was estimated using a molar extinction coefficient at 260 nm (S1 and S2, 881,375 $M^{-1}cm^{-1}$; S3; 769,475 $M^{-1}cm^{-1}$).

Monitoring library recovery

qPCR reactions (30 μL) were performed with the following reagent volumes: 15 μL of PerfeCTa SYBR Green FastMix for IQ (Quantabio, 95071-012), 3 μL of 5 μM forward primer, 3 μL of 5 μM reverse primer, 7.5 μL of water, and 1.5 μL of template. Samples were transferred to a CFX96 Touch Deep Well Real-Time PCR Detection System (Bio-Rad Laboratories, 1854095) and subjected to thermal cycling using a protocol of 95°C for 30s, 40 × (95°C, 15 s; 51°C, 30 s; 72°C, 30 s), and interrogating SYBR Green fluorescence after the anneal step of each cycle as previously described.[26] Raw fluorescence data were then analyzed using CFX Maestro software.

Aptamer library sequencing and analysis

DNA libraries recovered after each selection round described above and the original, naive library were subjected to PCR with the same protocol described above but with unmodified primers (S1 and S2, 5505 and 6160; S3, 6708 and 6895). The previously determined optimum number of cycles was used for each library to obtain unmodified duplex DNA. PCR product size and quality were assessed by sample analysis by electrophoresis through 10% polyacrylamide gels with post-staining using SYBR Gold (Invitrogen, S11494) at this point and just before sequencing. MinElute spin columns (Qiagen, 28204) were used to purify the PCR products. A Qubit HS Duplex DNA Quantification kit (Invitrogen, Q32851) and Qubit 3.0 Fluorometer (Invitrogen, Q33216) were used to quantify the concentration of the purified PCR product. For each library, 10 ng was used as input into the NEBNext Ultra II DNA Library Prep with Sample Purification Beads (NEB, E7103S). Volumes recommended by the manufacturer were halved, and, in the purification of adaptor-ligated DNA (step 3), Qiagen MinElute columns were used in place of beads. Libraries were barcoded using NEBNext Multiplex Oligos for Illumina (index primers set 1 and set 2) (NEB, E7335S and E7500S). Paired-end sequencing was performed (S1 and S2, 150 cycles; S3, 100 cycles) on a single lane of an Illumina MiSeq instrument with 30% PhiX spike.

Usearch was used to merge paired-end reads. Reads with a total quality score >0.5 were discarded.[39] SeqKit was used to create uniform forward reads.[40] AptaSUITE was used to filter any reads that did not contain both the forward and reverse primers within an error of 3 bases. AptaSUITE was also used to rank aptamers by their abundance and cluster the aptamers by sequence similarity (AptaCluster).[27]

Immunofluorescence staining and IncuCyte SX5 imaging

Cells were washed with wash buffer. Aptamer solution (200 nM aptamer in wash buffer) was heated at 95°C for 5 min and snap cooled on ice. Final aptamer solution (200 nM aptamer in wash buffer) was added to cells for 1 h at 37°C. Cells were washed three times with wash buffer and incubated with 3.7% formaldehyde for 15 min at room temperature. Cells were washed twice with wash buffer and incubated with streptavidin, Alexa Fluor 647 conjugate (Invitrogen, S21374) secondary stain at 1:500 dilution in DPBS for 1 h at room temperature. Cells were washed three times with DPBS and imaged with IncuCyte SX5 (Sartorius) at 20× magnification. Quantification of aptamer staining was analyzed using IncuCyte Basic Analyzer software. Confluence was analyzed under the classic confluence segmentation, adjustment set to 0.1 background-to-cell ratio with cleanup settings for "hole fill" at 50.00 μm^2 and "adjust size" at 3 pixels. Aptamer staining was quantified using the "surface fit" segmentation routine with a threshold set to 1.5,000 NIRCU. Individual images were then filtered for confluence levels (undifferentiated SH-SY5Y, minimum of 6.5%; differentiated SH-SY5Y, minimum of 13% and maximum of 85%). Blinded image data were also filtered for excess stain artifacts that impacted the fluorescence intensity measurement (undifferentiated SH-SY5Y, n = 34–78 replicate image fields per condition in multiple replicate wells; differentiated SH-SY5Y, n = 32–76 replicate image fields per condition in multiple replicate wells). The metric shown in figures as "relative fluorescence" was calculated as the integrated fluorescent intensity per image relative to the percentage confluence.

SH-SY5Y differentiation

Differentiation of SH-SY5Y cells used an optimized high-throughput protocol.[32] Prior to plating, cells were thawed and kept in a basic growth medium: DMEM:F12 (Gibco, 11330057) with 10% FBS (R&D Systems, S11550H), 1% penicillin-streptomycin (Gibco 15140122), and glutamax-I (Gibco, 35050061). Cells were seeded in the basic growth medium on dishes coated with 10 μg/mL Laminin (Corning, 354232). The next day (day 1 of differentiation) the medium was changed to stage I medium: DMEM with 2.5% FBS, 1% penicillin-streptomycin, glutamax-I, and 10 μM retinoic acid (Millipore Sigma, 554720). On day 4, medium was again changed to stage I medium. On days 6 and 9, the medium was changed to stage II medium: Neurobasal-A medium (Gibco, 10888022) with 1% penicillin-streptomycin, glutamax-I, 20 mM KCl (Sigma, S9638), 50 ng/mL brain-derived neurotrophic factor (R&D Systems, 11166BD010), and B-27 (Thermo Fisher Scientific, A3582801). Cells were used after day 11 of the differentiation process.

Human iPSC culture, maintenance, and iSN differentiation

The iPSC lines used for experimentation and the differentiation conditions used for obtaining sensory neurons have been described previously.[33,35] In brief, three iPSC lines created from the skin biopsies of individuals without health concerns were acquired from the Mayo Clinic Biotrust according to institutional review board (IRB)-approved protocol IRB #13-007298. The lines used in this study were reprogrammed from fibroblasts using Cytotune-iPS 2.0, and a single clone from each line that passed quality-control testing for karyotype analysis, pluripotency, and germ layer differentiation was used. iPSCs were maintained on LDEV-free Geltrex in mTeSR 1 and passaged using ReLeSR every 4 days.

Differentiation of iPSCs into sensory neurons (iSNs) used the dual-SMAD inhibition approach with modification.[41] iPSCs were dissociated into single cells using Accutase and plated as a monolayer (2×10^5 cells/cm^2) in mTeSR 1 supplemented with Y-27632. Differentiation was initiated 24 h post plating with a surface density of 80% confluence. The differentiation medium consisted of KSR medium, N2 medium, or a mixture of both. Days 0–4 included 100 nM LDN193189 and 10 μM SB431542 in the culture medium, and for days 2–10 the medium was supplemented with 3 μM CHIR99021, 10 μM DAPT, and 5 μM SU5402. Ten days post induction, neural crest derivatives were treated with mitomycin C (1 μg/mL) for 1 h. The following day, the neural crest derivatives were dissociated with Accutase and plated as single cells and small aggregates in neuronal medium for subsequent iSN maturation and maintenance (N2 supplemented with growth factors: 25 ng/mL NGF, BDNF, glial cell line-derived neurotrophic factor [GDNF], NT3, 0.5 mM cyclic AMP [cAMP], and 200 μM L-ascorbic acid). Typical iSN yields were in the range of 75%–90%. Maturity of iSNs using this approach has been characterized by protein marker expression at day 25,[35] RNA profiling, and electrophysiological behavior at day 30 and day 60.[33] iSN cultures contain a mixture of neural progenitors and nociceptors. Protein levels of ion channels, cell surface receptors, and synaptic vesicle proteins are suggestive of a functional nociceptor phenotype.

A complete list of materials and reagents used for human iPSC culture, maintenance, and iSN differentiation is provided in Table S3.

Colony-formation assay

SH-SH5Y cells were plated at 750 cells per well in 24-well plates (Falcon, 353047) and allowed to adhere for 24 h. Aptamer stock solutions for cell treatment (10× final indicated concentration) were prepared by heating and snap cooling in wash buffer and stored at −20°C or 4°C for the duration of the studies. Stock solutions (40 μL) were combined with growth medium (360 μL) to reach the indicated final aptamer concentration for daily treatments. Growth medium was replaced daily with 400 μL of fresh medium containing aptamer. Treatment continued for 13–14 days.

Medium was then aspirated from cells followed by gentle washing with PBS. Cells were then fixed in 100% methanol for 10 min at −20°C and immediately stained in 0.5% crystal violet (Sigma, C6158) for 10 min at −20°C. Cells were washed 3–5 times with water to remove excess staining solution before quantification of colony formation.

Optimizing biotinylated aptamer-streptavidin multimer stoichiometry

Stoichiometries of multimers of biotinylated aptamers bound to streptavidin were determined by holding aptamer concentration consistent at 1 μM and adding varying dilutions of streptavidin, Alexa Fluor 647 conjugate (Invitrogen, S21374) in wash buffer and incubating at room temperature for 1 h with end-to-end rotation. Multimer mixtures were analyzed by electrophoresis through 8% polyacrylamide gels in 0.5× TBE running buffer for 3.5 h at 250 V (26.25 V/cm) followed by imaging with an Amersham Typhoon laser-scanning platform (Cytiva).

Confocal imaging

Undifferentiated SH-SH5Y cells were plated on 35-mm glass-bottom dishes (MatTek, P35G-1.5-14-C) at 50%–70% confluency and incubated overnight at 37°C. Differentiated SH-SH5Y cells were plated on the same dishes and differentiated as described above before staining.

Biotinylated aptamers were incubated with fluorescently labeled streptavidin as described above prior to staining in all high-resolution images demonstrating aptamer binding (2% dilution of streptavidin). Cells on glass-bottom dishes were then gently washed twice in wash buffer before incubation with streptavidin-conjugated aptamer solutions for 1 h at 37°C. Cells were washed three times in wash buffer and then fixed in formaldehyde as performed in IncuCyte SX5 imaging studies.

Fixed cells were washed twice in PBS to remove excess formaldehyde and stained with Actin555 ReadyProbe (Invitrogen, R37112) diluted in PBS per manufacturer's recommendation for 30 min at room temperature. Cells were then washed twice more in PBS and stained with 1 μg/mL DAPI (Roche, 10236276001) in PBS for 5 min at room temperature. Plates were washed three times with PBS before imaging. Images were collected on a Zeiss LSM 780 confocal microscope.

Confluence and neurite measurements of aptamer-treated SH-SY5Y cells

SH-SY5Y cells were plated (50,000 cells/well) on 24-well plates (Falcon, 353047) and allowed to adhere for 24 h at 37°C. Aptamer stocks (10× concentration) were prepared in advance in wash buffer. Solutions were heated at 90°C for 5 min and snap cooled and stored at 4°C for the treatment period. Daily medium changes took place by replacing half of the volume of growth medium and dosing with aptamer to yield a final concentration of 350 nM in each well. This experiment continued for five medium changes and cells were imaged every 12 h with the Incucyte SX5 instrument.

Images were analyzed using the Incucyte Neurotrack software module (Sartorius, 9600-0010) for neurite measurements and the Basic Analyzer for confluence measurements. In the Neurotrack analyzer, the "cell-body cluster segmentation" mode was set to "brightness" with the "segmentation adjustment" value set to 1. The cleanup parameters were set to zero, with the "minimum cell width (μm)" set to 7.00. Neurite parameter filtering was set to "best," "neurite sensitivity" at 0.5, and "neurite width" at 1 μm.

Confluence was measured using the Basic Analyzer under the classic confluence segmentation mode with the segmentation adjustment set to 0.1. The cleanup settings were set to zero, "hole fill" set at 50.00 μm^2 and "adjust size" set at 3 pixels.

RNA-seq of aptamer-treated cells

SH-SY5Y cells were plated (100,000 cells/well) on six-well plates (Thermo Fisher Scientific, 353046) and allowed to adhere for 24 h. Aptamer stock solutions were prepared at 3.5 μM by heating and snap cooling in wash buffer and stored at 4°C for the duration of the treatment. Daily treatments were done by exchanging three-quarters of the well volume with aptamer diluted to 350 nM in growth medium. Treatments were carried out for 5 days before RNA extraction.

Growth medium was then removed and the PureLink RNA Mini Kit (Thermo Fisher Scientific, 12183018A) was used to extract RNA according to manufacturer recommendations for adherent mammalian cells. Genomic DNA was fragmented by passing lysate through a 20-gauge needle attached to an RNase-free syringe 10 times. Samples were then subjected to an on-column PureLink DNase treatment (Thermo Fisher Scientific, 12185010) to minimize genomic DNA contamination. Yield and sample quality were analyzed by nanodrop and Qubit RNA High Sensitivity Assay Kit (Thermo Fisher Scientific, Q32852). Sample yields were $\geq$2 μg at $\geq$50 ng/μL with A260/A280 purity ratio between 1.8 and 2.2 as recommended by Azenta Life Sciences.

Isolated RNA samples were stored at −80°C and transferred into RNA Stabilization Tubes (Azenta Life Sciences, GTR5025-GW) prior to sample submission. 40 μL of isolated RNA was added to tubes containing stabilization matrix, mixed thoroughly, and air dried in a biosafety hood for 24 h.

Isolated RNA was sequenced by Azenta Life Sciences. 50 million reads per sample were obtained in biological triplicates. Transcript sequences were aligned versus human genome assembly GRCh38.p14 and quantified with Salmon.[42,43] Differential expression analysis was performed with DESeq2 with Benjamini and Hochberg false discovery rate correction.[44] Volcano plots were generated with EnhancedVolcano.[45]

GO analysis of up- and downregulated transcript sets was performed by the Gene Ontology Resource in release 2023-11-15.[46–48] GSEA was performed in GSEA_4.3.2 using transcript quantification from Salmon.[49,50]

Human ESC-derived cortical neuron preparation

hESC-derived cortical neurons were generated using a protocol previously described.[34] All hESC work was conducted under an approved ESCRO protocol. Briefly, human embryonic stem cells were maintained in Essential 8 medium (Thermo) on Vitronectin-coated plates, passaged twice per week with EDTA, and tested negative for mycoplasma. All stem cell work was conducted according to protocols approved by the Tri-Institutional Stem Cell Initiative Embryonic Stem Cell Research Oversight Committee (Tri-SCI ESCRO). Excitatory neurons were generated using a protocol based on the previously described dual-SMAD inhibition paradigm.[51] Differentiations were initiated by dissociating hESC into single cells with Accutase and seeding at 300,000/cm^2 onto Matrigel-coated plates in Essential 8 medium with 10 μM Y-27632. Days 1–3 of the protocol consisted of Essential 6 medium (Thermo) supplemented with 10 μM SB431542 (Tocris) and 100 nM LDN193189 (Stemgent), and 2 μM Wnt inhibitor XAV-939 (Tocris) to promote anterior patterning.[52] Days 4–10 of the differentiation included only 10 μM SB431542 and 100 nM LDN193189. Days 11–20 of the differentiation included medium consisting of N2-supplemented DMEM/F12 and 1% GlutaMAX (Thermo). Cells received daily medium exchanges throughout the differentiation. On day 20, cells were dissociated in Accutase for 30 min and cryopreserved in STEM-CELLBANKER solution (Amsbio) at 10 million cells/vial. Neurons were thawed for experiments and plated on poly-L-ornithine and laminin-coated plates in low-glucose (5 mM) Neurobasal-A medium supplemented with 2% B27 (Thermo) and 1% GlutaMAX. During the first 7 days after plating, medium was supplemented with notch-inhibitor DAPT at 10 μM to promote any remaining progenitors transition toward the post-mitotic state. Following DAPT removal on D27, DNA aptamers were added to the medium at concentrations ranging from 10 pM to 10 nM. Cultures received medium changes twice per week after D20 replating in the specified medium conditions. Cells were fixed on D37 after 10 days of aptamer treatment.

hESC-derived cortical neuron immunostaining and high-content imaging analysis

Cells were fixed in 4% paraformaldehyde in PBS for 10 min at room temperature, permeabilized for 5 min in PBS with 0.1% Triton X-100, and blocked for 30 min in PBS with 5% normal goat serum (NGS). Incubation with primary antibodies was performed overnight at 4°C at the specified dilution in PBS with 2% NGS. Following five washes with PBS, cells were incubated with Alexa Fluor conjugated secondary antibodies (2 μg/mL) (Thermo) and DAPI for 30 min at room temperature. For biotin-conjugated aptamers, cells were stained with streptavidin, Alexa Fluor 647 conjugate (Invitrogen, S21374) at 1:500. Cells were washed five times in PBS before imaging.

Antibodies used were FOS (Abcam, ab208942, mouse, 1:500), MAP2 (Abcam, ab5392, chicken, 1:5,000), and NF-κB (Cell Signaling Technologies, 8242S, rabbit, 1:300).

Images were captured on the InCell Analyzer 6000 HCA system (GE Healthcare), using the 20× objective at nine fields per well. Images were analyzed using the Signals Image Artist version 1.3.29 from Revvity.

DATA AND CODE AVAILABILITY

All data supporting the statements and conclusions made by the authors are included in the figures and in the supplemental information. RNA-seq data are available on NCBI GEO: GSE278187.

ACKNOWLEDGMENTS

This work was supported by NIH grant R35GM143949 (L.J.M.), DOD grant W81XWH-22-1-0313 (L.J.M.), an NSF graduate fellowship (B.W.), the Mayo Clinic Graduate School of Biomedical Sciences grant 1R01NS128087 core grant P30CA008748 (L.S.), and fellowship F31AG067709 (A.P.M.). The authors thank members of the Maher, Staff, and Studer laboratories. We acknowledge the Mayo Clinic Genome Analysis Core for their contributions. We would like to thank Clare Lewis, Jesse Barnes, and Ralph Garippa at the

MSKCC Genome Screening Core Facility for their help with the InCell 6000 high-content imager.

AUTHOR CONTRIBUTIONS

Conceptualization, K.P., A.E.W., and L.J.M.; funding acquisition, L.S., A.E.W., N.P.S., and L.J.M.; investigation, K.P., J.R., B.W., and A.P.M.; data analysis, K.P., J.R., B.W., A.P.M., S.C.L.H., and L.J.M.; visualization, K.P., J.R., B.W., and A.P.M.; writing – original draft, K.P. and J.R.; writing – review & editing, K.P., J.R., B.W., A.P.M., S.C.L.H., L.S., A.E.W., N.P.S., and L.J.M. All authors read and approved the final manuscript.

DECLARATION OF INTERESTS

L.S. is a scientific co-founder and consultant of Bluerock Therapeutics and DaCapo Brainscience.

SUPPLEMENTAL INFORMATION

Supplemental information can be found online at https://doi.org/10.1016/j.omtn.2024.102392.

REFERENCES

1. Castillo, M., Liu, K., Bonilla, L., and Rameshwar, P. (2007). The immune properties of mesenchymal stem cells. Int. J. Biomed. Sci. *3*, 76–80.
2. Jeong, C.H., Kim, S.M., Lim, J.Y., Ryu, C.H., Jun, J.A., and Jeun, S.S. (2014). Mesenchymal stem cells expressing brain-derived neurotrophic factor enhance endogenous neurogenesis in an ischemic stroke model. BioMed Res. Int. *2014*, 129145.
3. Wilkins, A., Kemp, K., Ginty, M., Hares, K., Mallam, E., and Scolding, N. (2009). Human bone marrow-derived mesenchymal stem cells secrete brain-derived neurotrophic factor which promotes neuronal survival *in vitro*. Stem Cell Res. *3*, 63–70.
4. Madigan, N.N., Staff, N.P., Windebank, A.J., and Benarroch, E.E. (2017). Genome editing technologies and their potential to treat neurologic disease. Neurology *89*, 1739–1748.
5. Petrou, P., Gothelf, Y., Argov, Z., Gotkine, M., Levy, Y.S., Kassis, I., Vaknin-Dembinsky, A., Ben-Hur, T., Offen, D., Abramsky, O., et al. (2016). Safety and Clinical Effects of Mesenchymal Stem Cells Secreting Neurotrophic Factor Transplantation in Patients With Amyotrophic Lateral Sclerosis: Results of Phase 1/2 and 2a Clinical Trials. JAMA Neurol. *73*, 337–344.
6. Feldman, E.L., Boulis, N.M., Hur, J., Johe, K., Rutkove, S.B., Federici, T., Polak, M., Bordeau, J., Sakowski, S.A., and Glass, J.D. (2014). Intraspinal neural stem cell transplantation in amyotrophic lateral sclerosis: phase 1 trial outcomes. Ann. Neurol. *75*, 363–373.
7. Mazzini, L., Gelati, M., Profico, D.C., Sgaravizzi, G., Projetti Pensi, M., Muzi, G., Ricciolini, C., Rota Nodari, L., Carletti, S., Giorgi, C., et al. (2015). Human neural stem cell transplantation in ALS: initial results from a phase I trial. J. Transl. Med. *13*, 17.
8. Kunbaz, A., Warrington, A.E., Perwein, M.K., Fereidan-Esfahani, M., and Rodriguez, M. (2018). A natural human monoclonal antibody protects from axonal injury in different CNS degenerative disease models. Future Neurol. *13*, 23–29.
9. Mitsunaga, Y., Ciric, B., Van Keulen, V., Warrington, A.E., Paz Soldan, M., Bieber, A.J., Rodriguez, M., and Pease, L.R. (2002). Direct evidence that a human antibody derived from patient serum can promote myelin repair in a mouse model of chronic-progressive demyelinating disease. Faseb. J. *16*, 1325–1327.
10. Perwein, M.K., Smestad, J.A., Warrington, A.E., Heider, R.M., Kaczor, M.W., Maher, L.J., 3rd, Wootla, B., Kunbaz, A., and Rodriguez, M. (2018). A comparison of human natural monoclonal antibodies and aptamer conjugates for promotion of CNS remyelination: where are we now and what comes next? Expet Opin. Biol. Ther. *18*, 545–560.
11. Warrington, A.E., Asakura, K., Bieber, A.J., Ciric, B., Van Keulen, V., Kaveri, S.V., Kyle, R.A., Pease, L.R., and Rodriguez, M. (2000). Human monoclonal antibodies reactive to oligodendrocytes promote remyelination in a model of multiple sclerosis. Proc. Natl. Acad. Sci. USA *97*, 6820–6825.
12. Warrington, A.E., Bieber, A.J., Van Keulen, V., Ciric, B., Pease, L.R., and Rodriguez, M. (2004). Neuron-binding human monoclonal antibodies support central nervous system neurite extension. J. Neuropathol. Exp. Neurol. *63*, 461–473.
13. Watzlawik, J.O., Kahoud, R.J., Ng, S., Painter, M.M., Papke, L.M., Zoecklein, L., Wootla, B., Warrington, A.E., Carey, W.A., and Rodriguez, M. (2015). Polysialic acid as an antigen for monoclonal antibody HIgM12 to treat multiple sclerosis and other neurodegenerative disorders. J. Neurochem. *134*, 865–878.
14. Wilbanks, B., Maher, L.J., 3rd, and Rodriguez, M. (2019). Glial cells as therapeutic targets in progressive multiple sclerosis. Expert Rev. Neurother. *19*, 481–494.
15. Xu, X., Denic, A., Jordan, L.R., Wittenberg, N.J., Warrington, A.E., Wootla, B., Papke, L.M., Zoecklein, L.J., Yoo, D., Shaver, J., et al. (2015). A natural human IgM that binds to gangliosides is therapeutic in murine models of amyotrophic lateral sclerosis. Dis. Model. Mech. *8*, 831–842.
16. Xu, X., Wittenberg, N.J., Jordan, L.R., Kumar, S., Watzlawik, J.O., Warrington, A.E., Oh, S.H., and Rodriguez, M. (2013). A patterned recombinant human IgM guides neurite outgrowth of CNS neurons. Sci. Rep. *3*, 2267.
17. Paz Soldan, M.M., Warrington, A.E., Bieber, A.J., Ciric, B., Van Keulen, V., Pease, L.R., and Rodriguez, M. (2003). Remyelination-promoting antibodies activate distinct Ca2+ influx pathways in astrocytes and oligodendrocytes: relationship to the mechanism of myelin repair. Mol. Cell. Neurosci. *22*, 14–24.
18. Nastasijevic, B., Wright, B.R., Smestad, J., Warrington, A.E., Rodriguez, M., and Maher, L.J., 3rd (2012). Remyelination induced by a DNA aptamer in a mouse model of multiple sclerosis. PLoS One *7*, e39595.
19. Perschbacher, K., Smestad, J.A., Peters, J.P., Standiford, M.M., Denic, A., Wootla, B., Warrington, A.E., Rodriguez, M., and Maher, L.J., 3rd (2015). Quantitative PCR analysis of DNA aptamer pharmacokinetics in mice. Nucleic Acid Therapeut. *25*, 11–19.
20. Heider, R.M., Smestad, J.A., Lemus, H.N., Wilbanks, B., Warrington, A.E., Peters, J.P., Rodriguez, M., and Maher, L.J., 3rd (2018). An Assay that Predicts In Vivo Efficacy for DNA Aptamers that Stimulate Remyelination in a Mouse Model of Multiple Sclerosis. Mol. Ther. Methods Clin. Dev. *9*, 270–277.
21. Smestad, J., and Maher, L.J., 3rd (2013). Ion-dependent conformational switching by a DNA aptamer that induces remyelination in a mouse model of multiple sclerosis. Nucleic Acids Res. *41*, 1329–1342.
22. Hosseini Shamili, F., Alibolandi, M., Rafatpanah, H., Abnous, K., Mahmoudi, M., Kalantari, M., Taghdisi, S.M., and Ramezani, M. (2019). Immunomodulatory properties of MSC-derived exosomes armed with high affinity aptamer toward mylein as a platform for reducing multiple sclerosis clinical score. J. Contr. Release *299*, 149–164.
23. Kovalevich, J., Santerre, M., and Langford, D. (2021). Considerations for the Use of SH-SY5Y Neuroblastoma Cells in Neurobiology. Methods Mol. Biol. *2311*, 9–23.
24. Xicoy, H., Wieringa, B., and Martens, G.J.M. (2017). The SH-SY5Y cell line in Parkinson's disease research: a systematic review. Mol. Neurodegener. *12*, 10.
25. Cheung, Y.T., Lau, W.K.W., Yu, M.S., Lai, C.S.W., Yeung, S.C., So, K.F., and Chang, R.C.C. (2009). Effects of all-trans-retinoic acid on human SH-SY5Y neuroblastoma as *in vitro* model in neurotoxicity research. Neurotoxicology *30*, 127–135.
26. Pearson, K., Doherty, C., Zhang, D., Becker, N.A., and Maher, L.J., 3rd (2022). Optimized quantitative PCR analysis of random DNA aptamer libraries. Anal. Biochem. *650*, 114712.
27. Hoinka, J., Backofen, R., and Przytycka, T.M. (2018). AptaSUITE: A Full-Featured Bioinformatics Framework for the Comprehensive Analysis of Aptamers from HT-SELEX Experiments. Mol. Ther. Nucleic Acids *11*, 515–517.
28. Zuker, M. (2003). Mfold web server for nucleic acid folding and hybridization prediction. Nucleic Acids Res. *31*, 3406–3415.
29. SantaLucia, J., Jr. (1998). A unified view of polymer, dumbbell, and oligonucleotide DNA nearest-neighbor thermodynamics. Proc. Natl. Acad. Sci. USA *95*, 1460–1465.
30. Wang, L., Bing, T., Liu, Y., Zhang, N., Shen, L., Liu, X., Wang, J., and Shangguan, D. (2018). Imaging of Neurite Network with an Anti-L1CAM Aptamer Generated by Neurite-SELEX. J. Am. Chem. Soc. *140*, 18066–18073.
31. Chen, J., Liu, J., Wang, J., Zhang, Y., Wang, X., and Zhou, N. (2022). Fluorescent biosensor based on FRET and catalytic hairpin assembly for sensitive detection of polysialic acid by using a new screened DNA aptamer. Talanta *242*, 123282.

32. Dravid, A., Raos, B., Svirskis, D., and O'Carroll, S.J. (2021). Optimised techniques for high-throughput screening of differentiated SH-SY5Y cells and application for neurite outgrowth assays. Sci. Rep. *11*, 23935.

33. Ankam, S., Rovini, A., Baheti, S., Hrstka, R., Wu, Y., Schmidt, K., Wang, H., Madigan, N., Koenig, L.S., Stelzig, K., et al. (2019). DNA methylation patterns in human iPSC-derived sensory neuronal differentiation. Epigenetics *14*, 927–937.

34. Hergenreder, E., Minotti, A.P., Zorina, Y., Oberst, P., Zhao, Z., Munguba, H., Calder, E.L., Baggiolini, A., Walsh, R.M., Liston, C., et al. (2024). Combined small-molecule treatment accelerates maturation of human pluripotent stem cell-derived neurons. Nat. Biotechnol. *42*, 1615.

35. Hrstka, S.C.L., Ankam, S., Agac, B., Klein, J.P., Moore, R.A., Narapureddy, B., Schneider, I., Hrstka, R.F., Dasari, S., and Staff, N.P. (2021). Proteomic analysis of human iPSC-derived sensory neurons implicates cell stress and microtubule dynamics dysfunction in bortezomib-induced peripheral neurotoxicity. Exp. Neurol. *335*, 113520.

36. Sheng, M., and Greenberg, M.E. (1990). The regulation and function of c-fos and other immediate early genes in the nervous system. Neuron *4*, 477–485.

37. Agrawal, N.K., Allen, P., Song, Y.H., Wachs, R.A., Du, Y., Ellington, A.D., and Schmidt, C.E. (2020). Oligonucleotide-functionalized hydrogels for sustained release of small molecule (aptamer) therapeutics. Acta Biomater. *102*, 315–325.

38. Hoffmann, L.F., Martins, A., Majolo, F., Contini, V., Laufer, S., and Goettert, M.I. (2023). Neural regeneration research model to be explored: SH-SY5Y human neuroblastoma cells. Neural Regen. Res. *18*, 1265–1266.

39. Edgar, R.C. (2010). Search and clustering orders of magnitude faster than BLAST. Bioinformatics *26*, 2460–2461.

40. Shen, W., Le, S., Li, Y., and Hu, F. (2016). SeqKit: A Cross-Platform and Ultrafast Toolkit for FASTA/Q File Manipulation. PLoS One *11*, e0163962.

41. Chambers, S.M., Qi, Y., Mica, Y., Lee, G., Zhang, X.J., Niu, L., Bilsland, J., Cao, L., Stevens, E., Whiting, P., et al. (2012). Combined small-molecule inhibition accelerates developmental timing and converts human pluripotent stem cells into nociceptors. Nat. Biotechnol. *30*, 715–720.

42. Martin, F.J., Amode, M.R., Aneja, A., Austine-Orimoloye, O., Azov, A.G., Barnes, I., Becker, A., Bennett, R., Berry, A., Bhai, J., et al. (2023). Ensembl 2023. Nucleic Acids Res. *51*, D933–D941.

43. Patro, R., Duggal, G., Love, M.I., Irizarry, R.A., and Kingsford, C. (2017). Salmon provides fast and bias-aware quantification of transcript expression. Nat. Methods *14*, 417–419.

44. Love, M.I., Huber, W., and Anders, S. (2014). Moderated estimation of fold change and dispersion for RNA-seq data with DESeq2. Genome Biol. *15*, 550.

45. Blighe, K., Rana, S., and Lewis, M. (2021). EnhancedVolcano: Publication-Ready Volcano Plots with Enhanced Colouring and Labeling (GitHub).

46. Ashburner, M., Ball, C.A., Blake, J.A., Botstein, D., Butler, H., Cherry, J.M., Davis, A.P., Dolinski, K., Dwight, S.S., Eppig, J.T., et al. (2000). Gene ontology: tool for the unification of biology. The Gene Ontology Consortium. Nat. Genet. *25*, 25–29.

47. Gene Ontology Consortium, Aleksander, S.A., Balhoff, J., Carbon, S., Cherry, J.M., Drabkin, H.J., Ebert, D., Feuermann, M., Gaudet, P., Harris, N.L., et al. (2023). The Gene Ontology knowledgebase in 2023. Genetics *224*, iyad031.

48. Thomas, P.D., Ebert, D., Muruganujan, A., Mushayahama, T., Albou, L.P., and Mi, H. (2022). PANTHER: Making genome-scale phylogenetics accessible to all. Protein Sci. *31*, 8–22.

49. Mootha, V.K., Lindgren, C.M., Eriksson, K.F., Subramanian, A., Sihag, S., Lehar, J., Puigserver, P., Carlsson, E., Ridderstråle, M., Laurila, E., et al. (2003). PGC-1alpha-responsive genes involved in oxidative phosphorylation are coordinately downregulated in human diabetes. Nat. Genet. *34*, 267–273.

50. Subramanian, A., Tamayo, P., Mootha, V.K., Mukherjee, S., Ebert, B.L., Gillette, M.A., Paulovich, A., Pomeroy, S.L., Golub, T.R., Lander, E.S., and Mesirov, J.P. (2005). Gene set enrichment analysis: a knowledge-based approach for interpreting genome-wide expression profiles. Proc. Natl. Acad. Sci. USA *102*, 15545–15550.

51. Chambers, S.M., Fasano, C.A., Papapetrou, E.P., Tomishima, M., Sadelain, M., and Studer, L. (2009). Highly efficient neural conversion of human ES and iPS cells by dual inhibition of SMAD signaling. Nat. Biotechnol. *27*, 275–280.

52. Tchieu, J., Calder, E.L., Guttikonda, S.R., Gutzwiller, E.M., Aromolaran, K.A., Steinbeck, J.A., Goldstein, P.A., and Studer, L. (2019). NFIA is a gliogenic switch enabling rapid derivation of functional human astrocytes from pluripotent stem cells. Nat. Biotechnol. *37*, 267–275.